N$_2$ activation on a molybdenum–titanium–sulfur cluster

Yasuhiro Ohki [1], Keisuke Uchida[1], Mizuki Tada[1,2], Roger E. Cramer[3], Takashi Ogura[4] & Takehiro Ohta [4]

The FeMo-cofactor of nitrogenase, a metal–sulfur cluster that contains eight transition metals, promotes the conversion of dinitrogen into ammonia when stored in the protein. Although various metal–sulfur clusters have been synthesized over the past decades, their use in the activation of N$_2$ has remained challenging, and even the FeMo-cofactor extracted from nitrogenase is not able to reduce N$_2$. Herein, we report the activation of N$_2$ by a metal–sulfur cluster that contains molybdenum and titanium. An N$_2$ moiety bridging two [Mo$_3$S$_4$Ti] cubes is converted into NH$_3$ and N$_2$H$_4$ upon treatment with Brønsted acids in the presence of a reducing agent.

[1] Department of Chemistry, Graduate School of Science, Nagoya University, Furo-cho, Chikusa-ku, Nagoya 464-8602, Japan. [2] Research Center for Materials Science and Integrated Research Consortium on Chemical Sciences, Nagoya University, Nagoya 464-8602, Japan. [3] Department of Chemistry, University of Hawaii, Honolulu, HI 96822, USA. [4] Picobiology Institute, Graduate School of Life Science, University of Hyogo, RSC-UH LP Center, Hyogo 679-5148, Japan. Deceased: Takashi Ogura. Correspondence and requests for materials should be addressed to Y.O. (email: ohki@chem.nagoya-u.ac.jp)

Metal–sulfur clusters are a ubiquitous class of inorganic compounds, and span a wide range of structural and electronic features[1,2]. One unique function of protein-supported clusters is the conversion of N_2 into NH_3, which is mediated by the FeMo-cofactor of nitrogenase (Fig. 1a)[3–5]. The FeMo-cofactor can be extracted from the protein into organic solvents without significant degradation of its metal–sulfur core[6,7]. The extracted form catalyzes the reduction of non-native C_1 substrates, such as CO and CO_2 in the presence of reducing agents and protons to furnish CH_4 and short-chain hydrocarbons[8,9], and similar catalytic reductions can also be accomplished with the synthetic analog $[Cp^*MoFe_5S_9(SH)]^{3-}$ ($Cp^* = \eta^5\text{-}C_5Me_5$)[10]. However, N_2 cannot be reduced with the extracted FeMo-cofactor[7] or its synthetic analogs, highlighting the difference in N_2-reducing activity between the protein-supported FeMo-cofactor and discrete metal–sulfur clusters in solution. Thus, a molecular basis for the reduction of N_2 on metal–sulfur clusters remains elusive, while some aqueous suspensions or emulsions of Fe–S or Mo–Fe–S compounds have been found to generate NH_3[11–14] and some thiolate-supported Fe complexes have been found to activate N_2[15–17]. The cuboidal cluster $Cp^*_3Ir_3S_4Ru(tmeda)(N_2)$ (tmeda = tetramethylethylenediamine) is the only structurally characterized example for the binding of N_2 to a metal–sulfur cluster, although the conversion of the Ru-bound N_2 has not yet been achieved[18].

It should be noted that the structure of the FeMo-cofactor can be seen as a fused form of two cubes (Fig. 1b), implying the utility of cubes in the activation of N_2. However, synthetic examples are limited for the fused form of such metal–sulfur cubes[19–23], and a carbon-centered derivative still remains unprecedented. In order to develop a strategy for the activation of N_2 on synthetic metal–sulfur clusters, we examined independent cubes in this study. Our design (Fig. 2) is based on the trinuclear Mo–sulfur cluster platform $Cp^*_3Mo_3(\mu\text{-}S)_3(\mu_3\text{-}S)$ (**1**)[24] for the accommodation of a metal atom via three doubly bridging sulfur atoms to furnish a cubic structure. Ti was chosen as the additional metal to demonstrate the proof-of-concept, on the basis of successful examples of Ti complexes in N_2 chemistry[25], e.g. some recent studies on the activation of N_2 mediated by Ti–hydride complexes[26,27]. The resulting $[Mo_3S_4Ti]$ cluster (Fig. 2, top right) is reduced in the presence of N_2, to generate a Ti-based reaction site for the activation of N_2. Herein, we report the activation of N_2, as well as its conversion into NH_3 and N_2H_4, on a Mo–Ti–S cluster.

Results and Discussion

Synthesis of a cubic $[Mo_3S_4Ti]$ cluster and an N_2-cluster. The cubic $[Mo_3S_4Ti]$ precursor cluster $Cp^*_3Mo_3S_4TiCl_2$ (**2**) was synthesized in 70% yield in tetrahydrofuran (THF) from the reaction of in situ generated $[\textbf{1}]^-$ with $TiCl_3(THF)_3$ (Fig. 2), in a manner similar to the synthesis of cubic clusters from trinuclear Mo–sulfur clusters[28,29]. The molecular structure of **2** (Supplementary Figure 1 and Supplementary Table 3) reveals a nearly square-pyramidal geometry of titanium with an apical sulfur atom, where the $Ti\text{-}S_{apical}$ distance (2.2799(7) Å) is shorter than the $Ti\text{-}S_{basal}$ distances (2.3888(6) and 2.4272(6) Å). The Ti–Cl distances (2.3429(7) and 2.3812(7) Å) are close to those in a Ti(III) complex (average 2.353(4) Å) supported by three chlorides and a tridentate phosphine ligand[30]. The reduction of **2** with potassium graphite (KC_8) in THF under an atmosphere of N_2 resulted in the coordination and reduction of N_2 to form the brown cluster $[K(THF)_2]_2[Cp^*_3Mo_3S_4Ti]_2(\mu\text{-}N_2)$ (**3**) in 60% yield, in which an N_2 moiety bridges two $[Mo_3S_4Ti]$ cubes via binding to the Ti atoms. Product(s) of analogous reactions under atmospheres of H_2 or Ar have not been characterized so far. Cluster **3**
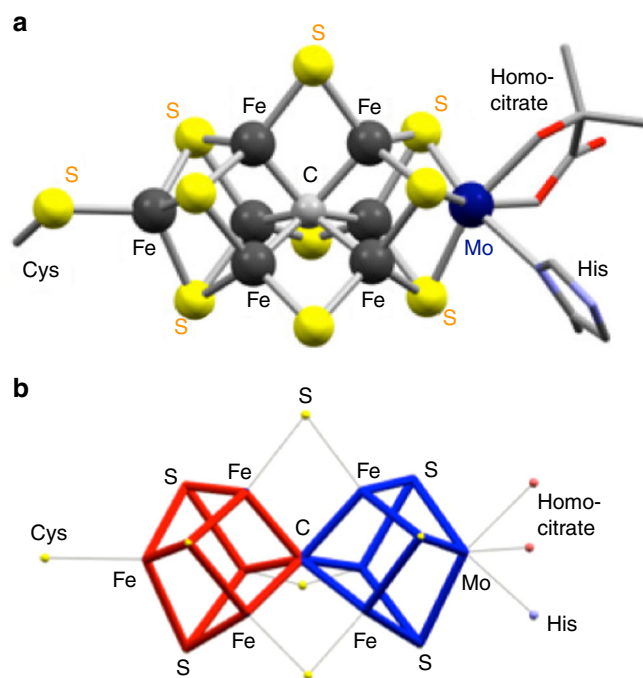
Fig. 1 Structure of the nitrogenase FeMo-cofactor. **a** The resting-state structure. The peptide chains of cysteine (Cys) and histidine (His), as well as a part of (*R*)-homocitrate are omitted for clarity. Color legend: C, gray; Fe, black; Mo, dark blue; S, yellow; O, red; N, light blue. **b** Wire-frame drawing of the inorganic part of the FeMo-cofactor, which highlights the fused form of the two cubes

is diamagnetic, and the ^{15}N NMR spectrum of ^{15}N-labeled **3** exhibited a signal at −75.4 ppm relative to CH_3NO_2 in THF-d_8 (Supplementary Figure 5). A single-crystal X-ray diffraction analysis of **3** established that N_2 is linearly aligned with the two Ti atoms to form a $Ti\text{-}N{=}N\text{-}Ti$ moiety (Fig. 3 and Supplementary Figure 4). Its N–N distance (1.294(7) Å) is comparable to the longest bonds reported for $Ti\text{-}N{=}N\text{-}Ti$ complexes[31–33], suggesting a high degree of N_2 reduction. The N–N distance in **3** is slightly longer than that in $H_3CN{=}NCH_3$ (1.25 Å)[34], but shorter than that in $H_2N\text{-}NH_2$ (1.46 Å)[25], indicating a character between $N{=}N$ double and N–N single bonds for the bridging N_2 in **3**. This notion was supported by resonance-Raman spectroscopy (Fig. 4 and Supplementary Figure 8), which showed a ν_{NN} band of **3** at 1240 cm^{-1} based on the difference spectrum of **3** and ^{15}N-labeled **3**. This ν_{NN} frequency falls between those of $H_3CN{=}NCH_3$ (1575 cm^{-1})[35] and $H_2N\text{-}NH_2$ (1111 cm^{-1})[36]. The observed shift (40 cm^{-1}) between **3** (1240 cm^{-1}) and ^{15}N-labeled **3** (1200 cm^{-1}) is consistent with the calculated shift (42 cm^{-1}) for the replacement of $^{14}N_2$ by $^{15}N_2$ assuming a diatomic harmonic oscillator.

Owing to the robust Cp^*–Mo and Mo–S bonds in the present system, we speculate that the three Mo atoms remain intact during the activation of N_2, leaving Ti as the reaction site in each cube. These robust bonds would also help to avoid the degradation of the cubic structure by aggregation or fragmentation.

Conversion of the N_2 moiety into NH_3 and N_2H_4. The high degree of reduction in **3** prompted us to attempt a stoichiometric conversion of the coordinated N_2 into NH_3 and N_2H_4. Upon treatment of **3** with protons from either H_2O or HCl, the color changed from brown to green, and NH_3, N_2H_4, and $[\textbf{1}]^+$ were detected. The resulting products NH_3 and N_2H_4 were quantified by indophenol and azo-dye titration methods, respectively
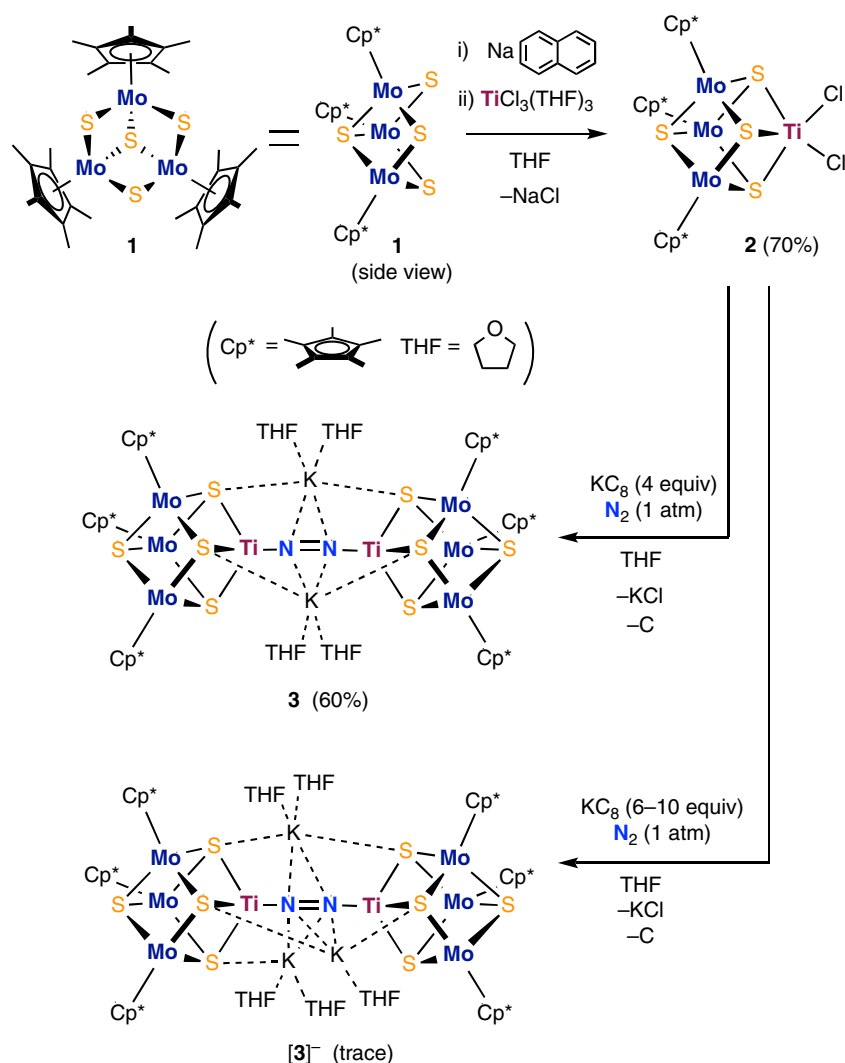
Fig. 2 Reactions in this study. Synthesis of the cubic [Mo_3S_4Ti] cluster **2**, the N_2-binding cluster **3**, and its 1e reduced form [**3**]⁻; Cp* = η⁵-pentamethylcyclopentadienyl; THF tetrahydrofuran
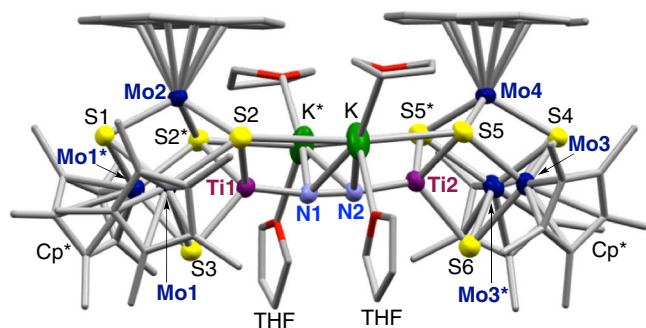
Fig. 3 Molecular structure of the N_2 cluster **3**. For clarity, carbon and oxygen atoms are drawn as capped sticks, while other atoms are drawn with thermal ellipsoids set at 50% probability. Color legend: C, gray; Mo, dark blue; Ti, purple; S, yellow; O, red; N, light blue; K, green. Selected bond distances (Å): N1–N2 1.294(7), Mo1–Mo1* 2.6766(8), Mo1–Mo2 2.8853(6), Mo3–Mo3* 2.7392(8), Mo3–Mo4 2.8518(6), Mo1–Ti1 3.0315(10), Mo2–Ti1 3.0908(12), Mo3–Ti2 3.0301(10), Mo4–Ti2 3.0778(12), Ti1–N1 1.802(5), Ti2–N2 1.798(5), K–N1 2.797(3), K–N2 2.782(3)
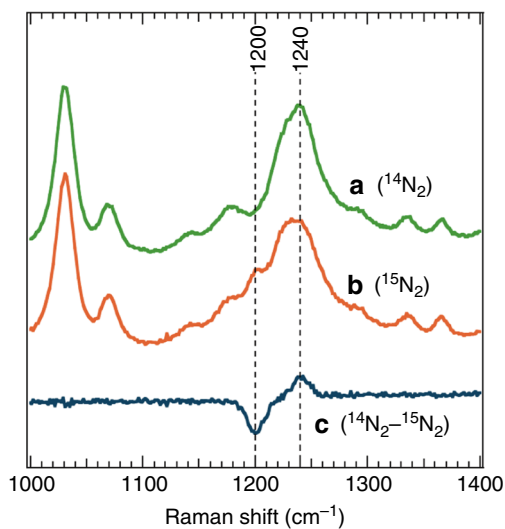
Fig. 4 Spectroscopic characterization of the Ti-N≡N-Ti moiety. Resonance-Raman spectra for **3** (**a**, green line) and ¹⁵N-labeled **3** (**b**, orange line), as well as their difference spectrum (**c**, dark blue line) in THF at −30 °C

Table 1 Protonation of 3 in the presence/absence of KC₈[a]

Entry	Proton source	KC_8 (equiv)	NH_3 (equiv)	N_2H_4 (equiv)
1	H_2O	0	0.12(3)	0.60(3)
2	H_2O	6	0.47(27)	0.56(10)
3	H_2O	100	1.20(19)	n.d.[b]
4	HCl	0	0.29(5)	0.12(10)
5	HCl	6	0.43(15)	0.19(6)
6	HCl	100	0.20(8)	n.d.[b]

[a] Yields represent the average of three runs. Standard deviations are given in parentheses
[b] n.d. = not detected

(Supplementary Tables 1 and 2)[37,38]. As summarized in Table 1 (entries 1 and 4), small to moderate amounts of NH_3 (0.12 (3)–0.29(5) equiv) and N_2H_4 (0.12(10)–0.60(3) equiv) were detected by protonation of **3** with an excess H_2O or HCl. While the length of the N–N bond in **3** indicates that a reduction has occurred, additional electrons are required for the cleavage of the N–N bond to form NH_3. Therefore **3** was treated with KC_8 and H_2O or HCl. In the presence of 6 equiv of KC_8, the average amount of NH_3 generated by protonation with H_2O increased from 0.12(3) to 0.47(27) equiv (entry 5), while the fluctuations observed allow only a cautious comparison. The NH_3 yields in entries 4 and 5 (HCl) are comparable and within error. The yields of N_2H_4 in entries 2 (0.56(10) equiv from H_2O) and 5 (0.19(6) equiv from HCl) remained comparable to those of reactions in the absence of KC_8. The formation of N_2H_4 from the Ti–N=N–Ti moiety is reasonable, as this N–N bond exhibits an N=N double and N–N single bond character. In the presence of 0–6 equiv of KC_8, subsequent protonation by H_2O provided approximately three times the amount of N_2H_4 than the reactions with HCl. Such acid-dependent selectivity may arise from the affinities of the conjugate bases (OH⁻ or Cl⁻) toward metals, where the high oxophilicity of the Ti and K atoms can facilitate the coordination of H_2O onto these atoms, which could lead to an efficient protonation of the neighboring Ti–N=N–Ti moiety.

Even in the presence of a slight excess (6 equiv) of KC_8, conversion of the N_2 moiety of **3** into NH_3 was not complete and notable amounts of N_2H_4 were detected (entries 2 and 5). These results indicate that some of the added KC_8 remains unreacted with the N_2 cluster and is subsequently quenched directly by H_2O or HCl. However, the formation of N_2H_4 was suppressed when a large excess of KC_8 was added prior to protonation (entries 3 and 6). While the protonation with HCl did not increase the amount of NH_3 (entry 6), the maximum yield of NH_3 (1.20(19) equiv) was achieved when 100 equiv KC_8 were added prior to the protonation with H_2O (entry 3). When conditions identical to those of entry 3 were applied for the ¹⁵N-enriched **3** under an atmosphere of ¹⁴N₂, the ¹H NMR spectrum of the resulting ammonium salt indicated the exclusive formation of ¹⁵NH₃, which originates from the Ti–¹⁵N=¹⁵N–Ti moiety (Supplementary Figure 15). After addition of an excess of protons to **3**, the Ti atom probably dissociates from the [Mo₃S₄Ti] cube, which is supported by the appearance of an intense signal of [**1**]⁺ in the electro-spray ionization mass (ESI-MS) spectrum of the resulting mixture (Supplementary Figure 16) and the color change of the mixture from dark brown to green. Thus, at this stage, the possibility of N_2 functionalization after dissociation of the Ti atom cannot be ruled out unequivocally.

It has been reported that metal–sulfur clusters exhibit stability across various oxidation states, which allows the storage and transportation of electrons[39,40]. It is therefore worthy of notice that the 1e-reduced cluster [**3**]⁻ was obtained in trace amounts from the reaction of **2** with 6–10 equiv of KC_8 under an atmosphere of N_2 (Fig. 2, bottom). The characterization of [**3**]⁻

was carried out only by ¹H NMR and crystallographic analysis due to the trace amounts available. Cluster [**3**]⁻ is paramagnetic and its ¹H NMR spectrum in THF-d_8 exhibited a broad Cp* signal at 5.84 ppm (Supplementary Figure 10). The molecular structure of [**3**]⁻ (Supplementary Figure 9) revealed an interaction of three potassium ions with the bridging N_2 moiety, where the N–N distance (1.293(5) Å) is comparable to that in **3** (1.294(7) Å). A structural comparison between the [Mo₃S₄Ti] cubes of **3** and [**3**]⁻ reveals the elongation of distances in [**3**]⁻. In detail, a relatively large contribution of the metal atoms for the storage of the additional electron is indicated by the larger differences in the average distances of Mo–Ti (3.0487(12) Å for **3** and 3.0242(8) Å for [**3**]⁻) and Mo–Mo (2.8150(8) Å for **3** and 2.8668(6) Å for [**3**]⁻), rather than the average metal–sulfur distances, i.e. Mo–S (2.3952(16) Å for **3** and 2.3966(11) Å for [**3**]⁻), and Ti–S (2.328 (2) Å for **3** and 2.3297(13) Å for [**3**]⁻). The detailed reaction pathways for the formation of NH_3 and N_2H_4 from **3** or [**3**]⁻ remain unclear at this point, as the dissociation of the Ti atom from the [Mo₃S₄Ti] cube renders the identification of possible cluster intermediates difficult.

In summary, we successfully achieved the activation of N_2 and its conversion into sub-stoichiometric mixtures of NH_3 and N_2H_4 on synthetic Mo–Ti–S cubes by selectively generating the Ti-based reaction sites. This work thus represents a step towards the assembly of structural and functional models for the FeMo-cofactor.

Methods

General procedure. All reactions and manipulations were carried out under an atmosphere of nitrogen using standard Schlenk line or glove box techniques. Solvents for reactions were purified by passing over columns of activated alumina and a supported copper catalyst. TiCl₃(THF)₃[41], [Cp*₃Mo₃S₄][PF₆] ([**1**]⁺)[42], and KC₈[43] were prepared according to literature procedures. All other reagents were purchased from common commercial sources and used without further purification. General considerations on the measurements and experiments as well as some experimental details are described in the Supplementary Methods.

Modified synthesis of Cp*₃Mo₃S₄ (1). Compound **1** was originally synthesized from the reaction of Cp*Mo(StBu)₃ (tBu = tert-butyl) with Na/Hg[24], but this reaction is not ideally suitable for a gram-scale synthesis. Instead, cluster **1** was synthesized on a multi-gram scale through the reduction of [**1**]⁺. For that purpose, KC₈ (1.36 g, 10.06 mmol) was added in portions to a THF (150 mL) suspension of [**1**]⁺ (9.78 g, 10.12 mmol) at room temperature. After stirring this mixture overnight, the solvent was removed under reduced pressure. The residue was extracted four times with toluene (350 mL). The extract was stored at −30 °C to precipitate green blocks of **1**. The mother liquor was concentrated to ca. 1/5 of the original volume and stored at −30 °C to obtain a second crop. The total amount of green crystals of **1** was 6.17 g (7.51 mmol, 83%). This product was characterized by comparison with ¹H NMR data in the literature[24]. ¹H NMR (C₆D₆): δ 8.56 ($w_{1/2}$ = 14 Hz, Cp*).

Synthesis of Cp*₃Mo₃S₄TiCl₂ (2). A THF (20 mL) solution of **1** (1.00 g, 1.22 mmol) was cooled to −100 °C, and a THF solution of sodium naphthalenide (19.5 mM, 62 mL, 1.21 mmol) was added. The reaction mixture was gradually warmed to room temperature to give a dark green solution. The mixture was again cooled to −100 °C, and TiCl₃(THF)₃ (451 mg, 1.22 mmol) was added. The reaction mixture was warmed to room temperature and stirred for 5 days, affording a dark brown suspension. After concentration to ca. 5 mL under reduced pressure, the mixture was cooled to −30 °C, which caused the precipitation of a dark brown powder. The supernatant was removed and the dark brown powder was washed with hexane (20 mL × 2). The brown powder was dissolved into CH₂Cl₂ (15 + 3 mL), and hexane (100 mL) was layered on top of this solution. The subsequent slow diffusion led to the formation of brown plates of Cp*₃Mo₃S₄TiCl₂·CH₂Cl₂ (**2**·CH₂Cl₂). These brown crystals were washed with hexane (15 mL × 2), and then dissolved in THF (15 mL). After stirring overnight, THF and CH₂Cl₂ were removed under reduced pressure to give a brown powder of **2** (801 mg, 0.854 mmol, 70%). ¹H NMR (CD₂Cl₂): δ 9.23 ($w_{1/2}$ = 8 Hz, Cp*); solution magnetic moment (CD₂Cl₂, 297 K): μ_{eff} = 1.3 μB; Cyclic voltammogram (2 mM in CH₂Cl₂, potential vs. (C₅H₅)₂Fe/[(C₅H₅)₂Fe]⁺): $E_{1/2}$ = −0.28, −1.34 V; UV/Vis (CH₂Cl₂): λ_{max} 415 nm (sh, 1200 cm⁻¹ M⁻¹), 753 nm (660 cm⁻¹ M⁻¹); analysis (calcd., found for C₃₀H₄₅Cl₂Mo₃S₄Ti): C (38.31, 38.77), H (4.82, 4.70), S (13.64, 13.24).

Synthesis of [K(THF)$_2$]$_2$[Cp*$_3$Mo$_3$S$_4$Ti]$_2$(μ-N$_2$) (3). Cluster **2** (200 mg, 0.213 mmol) and KC$_8$ (116 mg, 0.858 mmol) were charged into one side of an H-shaped glass vessel (Supplementary Fig. 3). The other arm of the vessel was charged with THF (10 mL), which was vacuum-transferred to the solid mixture at 78 K. The vessel was filled with N$_2$ (1 atm) and then sealed. The mixture was slowly warmed using a methanol/liquid N$_2$ slurry. Stirring of the mixture with a magnetic stirring bar was initiated, once part of frozen THF had melted. The mixture was gradually warmed to room temperature, giving a dark red-brown suspension. Stirring was continued overnight, before the solvent was removed under reduced pressure and the residue was extracted with THF (50 mL). The solution was filtered, concentrated to ca. 3 mL, and stored at −30 °C. Cluster **3** (136 mg, 0.064 mmol, 60%) was obtained as dark-brown crystalline blocks, which were washed with pentane. ^{1}H NMR (THF-d_8): δ 1.70 (Cp*); ^{13}C{^{1}H} NMR (THF-d_8): δ 13.6 (C$_5$Me$_5$), 96.3 (C$_5$Me$_5$); UV/Vis (THF): λ_{max} 356 nm (35800 cm$^{−1}$ M$^{−1}$), 500 nm (15,800 cm$^{−1}$ M$^{−1}$); Resonance-Raman spectrum (0.07 mM in THF, λ_{ex} 355 nm, −30 °C): 1240 cm$^{−1}$ (ν_{NN}); analysis (calcd., found for C$_{76}$H$_{122}$K$_2$Mo$_6$N$_2$O$_4$S$_8$Ti$_2$): C (42.78, 42.36), H (5.76, 5.80), N (1.31, 1.37), S (12.02, 12.27).

Synthesis of ^{15}N$_2$-labeled 3. This cluster was synthesized in a manner similar to that of **3**, using cluster **2** (173 mg, 0.184 mmol), KC$_8$ (100 mg, 0.740 mmol), and ^{15}N$_2$ (1 atm). Crystals of ^{15}N$_2$-labeled **3** were obtained in 60% yield (117 mg, 0.055 mmol). ^{15}N{^{1}H} NMR (THF-d_8, referenced to external CH$_3$NO$_2$): δ −75.4; Resonance-Raman spectrum (THF, −30 °C): 1200 cm$^{−1}$ (ν_{NN}).

References

1. Krebs, B. & Henkel, G. Transition-metal thiolates: from molecular fragments of sulfide solids to models for active centers in biomolecules. *Angew. Chem. Int. Ed. Engl.* **30**, 769–788 (1991).
2. Holm, R. H. & Lo, W. Structural conversions of synthetic and protein-bound iron-sulfur clusters. *Chem. Rev.* **116**, 13685–13713 (2016).
3. Hoffman, B. M., Lukoyanov, D., Yang, Z. –Y., Dean, D. R. & Seefeldt, L. C. Mechanism of nitrogen fixation by nitrogenase: the next stage. *Chem. Rev.* **114**, 4041–4062 (2014).
4. Spatzal, T. et al. Evidence for interstitial carbon in nitrogenase FeMo cofactor. *Science* **334**, 940 (2011).
5. Lancaster, K. M. et al. X-ray emission spectroscopy evidences a central carbon in the nitrogenase iron–molybdenum cofactor. *Science* **334**, 974–977 (2011).
6. Shah, V. K. & Brill, W. J. Isolation of an iron-molybdenum cofactor from nitrogenase. *Proc. Natl Acad. Sci. USA* **74**, 3249–3253 (1977).
7. Smith, B. E. et al. Exploring the reactivity of the isolated iron-molybdenum cofactor of nitrogenase. *Coord. Chem. Rev.* **185–186**, 669–687 (1999).
8. Lee, C. C., Hu, Y. & Ribbe, M. W. ATP-independent formation of hydrocarbons catalyzed by isolated nitrogenase cofactors. *Angew. Chem. Int. Ed.* **51**, 1947–1949 (2012).
9. Hu, Y. & Ribbe, M. W. Nitrogenases—a tale of carbon atom(s). *Angew. Chem. Int. Ed.* **55**, 8216–8226 (2016).
10. Tanifuji, K. et al. Structure and reactivity of an asymmetric synthetic mimic of nitrogenase cofactor. *Angew. Chem. Int. Ed.* **55**, 15633–15636 (2016).
11. Dörr, M. et al. A possible prebiotic formation of ammonia from dinitrogen on iron sulfide surfaces. *Angew. Chem. Int. Ed.* **42**, 1540–1543 (2003).
12. Tanaka, K., Hozumi, Y. & Tanaka, T. Dinitrogen fixation catalyzed by the reduced species of [Fe$_4$S$_4$(SPh)$_4$]$^{2−}$ and [Mo$_2$Fe$_6$S$_8$(SPh)$_9$]$^{3−}$. *Chem. Lett.* **11**, 1203–1206 (1982).
13. Banerjee, A. et al. Photochemical nitrogen conversion to ammonia in ambient conditions with FeMoS-chalcogels. *J. Am. Chem. Soc.* **137**, 2030–2034 (2015).
14. Liu, J. et al. Nitrogenase-mimic iron-containing chalcogels for photochemical reduction of dinitrogen to ammonia. *Proc. Natl Acad. Sci. USA* **113**, 5530–5535 (2016).
15. Čorić, I. et al. Binding of dinitrogen to an iron-sulfur carbon site. *Nature* **526**, 96–99 (2015).
16. Takaoka, A., Mankad, N. P. & Peters, J. C. Dinitrogen complexes of sulfur-ligated iron. *J. Am. Chem. Soc.* **133**, 8440–8443 (2011).
17. Creutz, S. E. & Peters, J. C. Diiron bridged-thiolate complexes that bind N$_2$ at the Fe^{II}Fe^{II}, Fe^{II}Fe^{I}, and Fe^{I}Fe^{I} redox states. *J. Am. Chem. Soc.* **137**, 7310–7313 (2015).
18. Mori, H., Seino, H., Hidai, M. & Mizobe, Y. Isolation of a cubane-type metal sulfido cluster with a molecular nitrogen ligand. *Angew. Chem. Int. Ed.* **46**, 5431–5434 (2007).
19. Lee, S. C. & Holm, R. H. The clusters of nitrogenase: synthetic methodology in the construction of weak-field clusters. *Chem. Rev.* **104**, 1135–1157 (2004).
20. Ohki, Y. & Tatsumi, K. New synthetic routes to metal-sulfur clusters relevant to the nitrogenase metallo-clusters. *Z. Anorg. Allg. Chem.* **639**, 1340–1349 (2013).
21. Zhang, Y., Zuo, J. L., Zhou, H. C. & Holm, R. H. Rearrangement of symmetrical dicubane clusters into topological analogues of the P cluster of nitrogenase: nature's choice? *J. Am. Chem. Soc.* **124**, 14292–14293 (2002).
22. Ohki, Y., Ikagawa, Y. & Tatsumi, K. Synthesis of new [8Fe-7S] clusters: a topological link between the core structures of P-cluster, FeMo-co, and FeFe-co of nitrogenases. *J. Am. Chem. Soc.* **129**, 10457–10465 (2007).
23. Ohki, Y. et al. Synthesis, structures, and electronic properties of [8Fe-7S] cluster complexes modeling the nitrogenase P-cluster. *J. Am. Chem. Soc.* **131**, 13168–13178 (2009).
24. Cramer, R. E., Yamada, K., Kawaguchi, H. & Tatsumi, K. Synthesis and structure of a Mo$_3$S$_4$ cluster complex with seven cluster electrons. *Inorg. Chem.* **35**, 1743–1746 (1996).
25. Fryzuk, M. D. & Johnson, S. A. The continuing story of dinitrogen activation. *Coord. Chem. Rev.* **200-202**, 379–409 (2000).
26. Shima, T. et al. Dinitrogen cleavage and hydrogenation by a trinuclear titanium polyhydride complex. *Science* **340**, 1549–1552 (2013).
27. Wang, B. et al. Dinitrogen activation by dihydrogen and a PNP-ligated titanium complex. *J. Am. Chem. Soc.* **139**, 1818–1821 (2017).
28. Shibahara, T. Syntheses of sulphur-bridged molybdenum and tungsten coordination compounds. *Coord. Chem. Rev.* **123**, 73–147 (1993).
29. Hidai, M., Kuwata, S. & Mizobe, Y. Synthesis and reactivities of cubane-type sulfido clusters containing noble metals. *Acc. Chem. Res.* **33**, 46–52 (2000).
30. Baker, R. J. et al. Early transition metal complexes of triphosphorus macrocycles. *Eur. J. Inorg. Chem.* 1975–1984 (2002).
31. Duchateau, R., Gambarotta, S., Beydoun, N. & Bensimon, C. Side-on versus end-on coordination of dinitrogen to titanium(II) and mixed-valence titanium(I)/titanium(II) amido complexes. *J. Am. Chem. Soc.* **113**, 8986–8988 (1991).
32. Chomitz, W. A., Sutton, A. D., Krinsky, J. L. & Arnold, J. Synthesis and reactivity of titanium and zirconium complexes supported by a multidentate monoanionic [N$_2$P$_2$] ligand. *Organometallics* **28**, 3338–3349 (2009).
33. Nakanishi, Y., Ishida, Y. & Kawaguchi, H. Nitrogen-carbon bond formation by reactions of a titanium-potassium dinitrogen complex with carbon dioxide, tert-butyl isocyanate, and phenylallene. *Angew. Chem. Int. Ed.* **56**, 9193–9197 (2017).
34. Almenningen, A., Anfinsen, I. M. & Haaland, A. An electron diffraction study of azomethane, CH$_3$NNCH$_3$. *Acta Chem. Scand.* **24**, 1230–1234 (1970).
35. Pearce, R. A. R., Levin, I. W. & Harris, W. C. Raman spectra and vibrational potential function of polycrystalline azomethane and azomethane-d$_6$. *J. Chem. Phys.* **59**, 1209–1216 (1973).
36. Gulaczyk, I., Kreglewski, M. & Valentin, A. The N-N stretching band of hydrazine. *J. Mol. Spectr.* **220**, 132–136 (2003).
37. Chaney, A. L. & Marbach, E. P. Modified reagents for determination of urea and ammonia. *Clin. Chem.* **8**, 130–132 (1962).
38. Watt, G. W. & Chrisp, J. D. A spectrophotometric method for the determination of hydrazine. *Anal. Chem.* **24**, 2006–2008 (1952).
39. Liu, J. et al. Metalloproteins containing cytochrome, iron−sulfur, or copper redox centers. *Chem. Rev.* **114**, 4366–4469 (2014).
40. Ohta, S. & Ohki, Y. Impact of ligands and media on the structure and properties of biological and biomimetic iron-sulfur clusters. *Coord. Chem. Rev.* **338**, 207–225 (2017).
41. Jones, N. A., Liddle, S. T., Wilson, C. & Arnold, P. L. Titanium(III) alkoxy-N-heterocyclic carbenes and a safe, low-cost route to TiCl$_3$(THF)$_3$. *Organometallics* **26**, 755–757 (2007).
42. Takei, I. et al. Synthesis of a new family of heterobimetallic tetranuclear sulfido clusters with Mo$_2$Ni$_2$S$_x$ (x = 4 or 5) or Mo$_3$M'S$_4$ (M' = Ru, Ni, Pd) cores. *Organometallics* **22**, 1790–1792 (2003).
43. Bergbreiter, D. E. & Killough, J. M. Reactions of potassium-graphite. *J. Am. Chem. Soc.* **100**, 2126–2134 (1978).

Author contributions

Y. O. conceived and designed the experiments; K. U. performed the experiments; T. O. and T. O. carried out the resonance Raman spectroscopic analysis; R. E. C. performed crystallographic analysis; M. T. participated in the discussion; Y. O. prepared the manuscript with input from all authors.

Additional information

Supplementary Information accompanies this paper at https://doi.org/10.1038/s41467-018-05630-6.

Competing interests: The authors declare no competing interests.

Reprints and permission information is available online at http://npg.nature.com/reprintsandpermissions/

Publisher's note: Springer Nature remains neutral with regard to jurisdictional claims in published maps and institutional affiliations.